

Computational Analysis Orifice Diameter Variations Effects of Conical Cavity Synthetic Jet Actuator on the Drag Force Reduction Percentage of the Reversed Ahmed Body Model

by Ramon Trisno_1

Submission date: 14-Oct-2019 10:03PM (UTC+0700)

Submission ID: 1192571334

File name: AIE_Laras-Computational_Analysis_Orifice_Diameter_Variations.pdf (1.03M)

Word count: 3053

Character count: 15126

3 Computational Analysis Orifice Diameter Variations Effects of Conical Cavity Synthetic Jet Actuator on the Drag Force Reduction Percentage of the Reversed Ahmed Body Model

7 Harinaldi¹, Ramon Trisno² and Dewi Larasati¹

¹Department Mechanical Engineering, Faculty of Engineering Universitas Indonesia, Kampus Baru Depo 16242

Abstract: This paper will discuss the simulation analysis of synthetic jet application effects on the Ahmed body model drag reduction. The purpose of this active airflow control is to improve the fuel consumption efficiency by reducing the wake area of the aerodynamic drag force. [1]Based on the fluid mechanic theory, the blow and the suction process of the membrane actuator of synthetic jet which produce vortex ring postpone the airflow separation in the rural area of the 70% reversed Ahmed body model. This phenomenon is believed that the vortex ring formation which formed by synthetic jet reduces the drag force by postponing the airflow separation. [2]The simulation is using k-Epsilon turbulence formulation feature on ANSYS student version software. Independent variables that applied on this simulation are the variation of the signal wave type, membrane vibration frequencies, and the airflow velocities. Types of signal waves are square, triangle, sinusoidal and frequencies ranges 90 Hz - 130 Hz with the frequency interval is 10 Hz. The free stream velocity is 60 km/hr which represent the maximum allowed city car speed on the urban street. The free variable is the orifice diameter of cavity variations; there are 3 mm, 5 mm and 8 mm. Based on the simulation result, 110 Hz square wave of membrane frequency is the boundary condition which resulting the maximum drag reduction at the 3 mm diameter of the conical synthetic jet in three different free stream velocities. The drag reduction percentage of 3 mm of orifice diameter synthetic jet when the free stream velocities 11 m/s, 13.9 m/s and 16.7 m/s are 14.20%, 18.62%, 12.47%.

Keywords: Active Control, Ahmed Body, CFD, Synthetic Jet

1. Introduction

1.1. Background

Indonesia government take action to reduce the greenhouse effect emission by 27% in 2022 (President rule No.61/21 about the action plan to reduce greenhouse gas effect) due to the data of International Energy Agency Outlook 2014 which concluded that the world greenhouse gas pollution would continuously increase up to 60% in 2030.

This inclining number of pollutant in the air is related to the rising number of the private transportation uses, based on the GAIKINDO data (national private car statistic data), the number of city car in Indonesia will increase up to 30% at the end of 2022.

Many of possible solutions provided to recover this problem despite reducing the amount of private city car. For example, giving an additional blowing-suction (synthetic jet actuator) devices to control the airflow separation in the rural area of the vehicle. [3]Based on the fluid mechanics theory, the postpone of airflow separation can reduce the wake area of air fluid. This phenomenon directly affects to declining percentage of the vehicle aerodynamic drag force, as the drag percentage minimise the amount of fuel to reach in certain distance required decreased.

These research purposes are analyzing the effect of orifice diameter variations of the synthetic jet actuator through the amount of drag force reduction by using ANSYS software. The numerical and visualization simulation result will provide in this following paper.

2. Simulation Method

2.1. Ahmed Body Model Design(AutoCAD)

Since this research is analyzing the drag force reduction on the city car model, so the 70% reversed Ahmed body model is the representation of the most city car model type. [4]

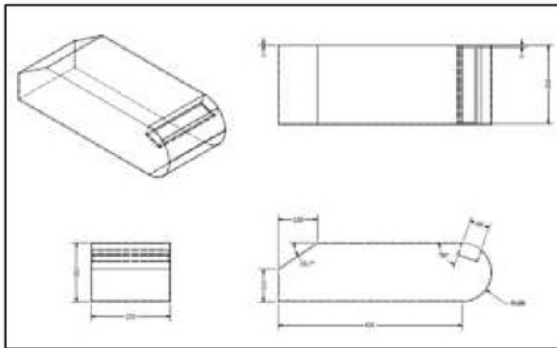


Fig. 1:70% Ahmed Body Model Design

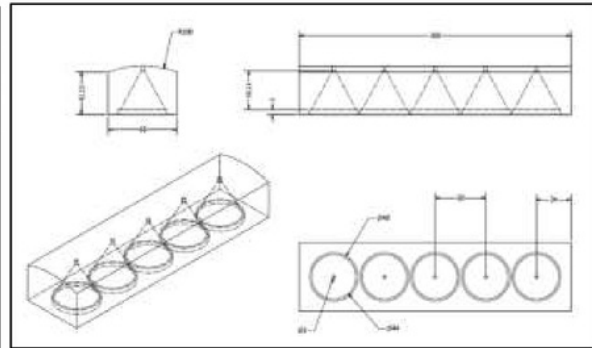


Fig. 2: Synthetic Jet Cavity 3 mm

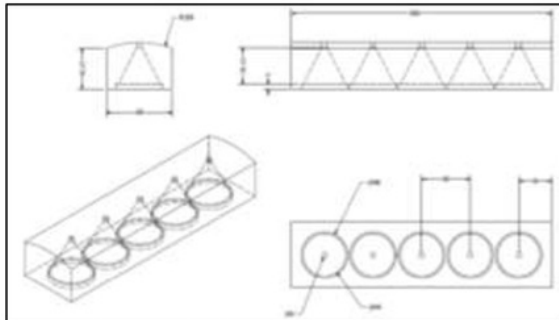


Fig. 3: Synthetic Jet Cavity 5 mm

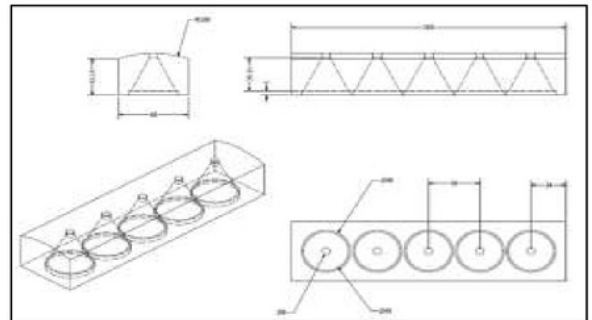


Fig. 4: Synthetic Jet Cavity Diameter 8 mm

2.2. Pre-Processing

First of all, it required to design the vehicle model and import the Computer Aided Design files to the design modeler in the CFD software with the format .igs. Here is the picture of the 2D model domain which can be seen in Fig.1. [5]

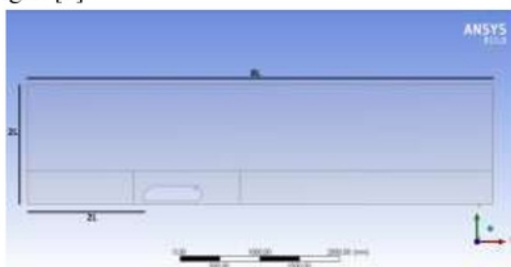


Fig. 5: 2D Model domain

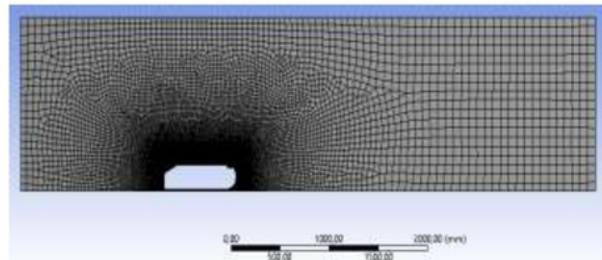


Fig. 6: Mesh Profile

Then, the process continues to make the mesh based on domain model dimension. Here the researcher using quadrilateral mesh type, because it has the highest calculation accuracy than another type of mesh shape type such as a triangle. [6] In order to make the simulation calculation more accurate on the Ahmed body model surfaces, it is necessary to set the inflation level of the meshing [7]. So as we can see from the Figure 6, the mesh profile is denser in the center of the domain than in the edge of domain profile.

Next step is setting the boundary condition for simulation. To be more specific, here is the specific parameter and boundary condition of simulation that is applied when setting the model mesh and input the fluid characteristic

TABLE I: Mesh Parameter

Parameter Mesh	
• Size Function	Proximity
• Relevance Center	Fine
• Initial Size Seed	Active Assembly
• Smoothing	High
• Transition	High
• Minimum Size	1 mm
• Maximum Size	100 mm
• Growth Size	1,2
• Minimum Edge Length	5 mm
• Nodes and Elements	16367 and 16011
• Element Quality	0,9323
• Aspect Ratio	1,134
• Jacobian Ratio	1,1289
• Skewness	0.58694
• Orthogonal Quality	0.98456

TABLE II: Boundary Conditions of the Model

Turbulence model	:	<i>K-Epsilon (2 Equation); Non-Equilibrium Wall Treatments</i>
Fluid Characteristic	:	
• Type	:	Udara
• Density	:	1.225 kg/m ³
• Viscosity	:	1.7894 x 10 ⁻⁵
Free stream profile	:	
• Inlet velocity	:	11,1 m/s; 13.9 m/s; 16,7 m/s
• Turbulence intensity	:	1%
• Turbulence viscosity ratio	:	10
Outlet profile	:	
• Outlet pressure	:	1 atm (Constant)
• Turbulence intensity	:	5%
• Turbulence viscosity ratio	:	10
Synthetic jet actuator boundary condition	:	UDF <i>Simusoidal, Triangle, 8 n Square wave</i> . Frequency: 90 Hz; 100 Hz; 110 Hz; 120 Hz; and 130 Hz.

2.3. Mesh Independencies

In this step, we need to determine which type and amount of mesh that will be used. The researcher tests the three type and amount of mesh element there are; 6000 elements coarse, 16000 elements, 30000 elements fine. The testing point is located at the surface where the high fluctuation of wind is high (80, 120)mm from the origin point (0,0).

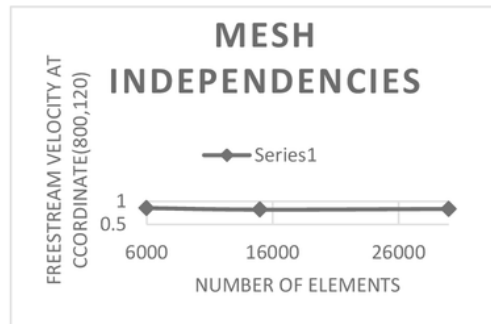


Fig. 7: Mesh Independencies

As it can be seen from the graph, the error percentage of 6000 coarse type mesh is 4% and it still acceptable to be used because the error is less than 5%. [8]

2.4. Solver

After all the mesh sets is finished, the simulation process continues to set the solution control parameter. To be more specific, the table below will explain more about the control that is used.

TABLE III: Solver Method

Solution Method	
<ul style="list-style-type: none"> Pressure-Velocity Coupling Scheme 	Coupled
<ul style="list-style-type: none"> Spatial Discretization <ul style="list-style-type: none"> Gradient Pressure Momentum Turbulent Kinetic Energy Turbulent Dissipation Rate 	Green-Gauss Node Based Standard Second Order Upwind Second Order Upwind Second Order Upwind

TABLE IV: Solution Control

Solution Control	
Flow Courant Number	50
Explicit Relaxation Factors <ul style="list-style-type: none"> Momentum Pressure 	0.25 0.25
Under Relaxation Factors <ul style="list-style-type: none"> Density Body Force Turbulent Kinetic Energy Turbulent Dissipation Rate Turbulent Viscosity Maximum Turbulent Viscosity Ratio 	1 1 0.8 0.8 0.8 10 ⁷

3. Simulation Result and Discussion

3.1. Vortex Ring Formation on The Synthetic Jet Cavity

In order to postpone the airflow separation on the rural area of synthetic jet, the qualities of air stroke output from orifice diameter is necessary to be considered. Based on the Holman criteria, in order to get maximum expulsion vortex ring formation, the parameter that needed to be fulfilled is:

$$\frac{1}{Sr} = \left(\frac{L_0/D}{\pi} \right) = \frac{U}{\omega D} = \frac{(UD/v)}{(\omega D^2/v)} = \frac{Reu}{S^2} > \tag{1}$$

The Reu/S^2 is get from the invers of Strouhal non-dimensional formula. L_0 is the stroke fluid which is forms from the orifice of synthetic jet, D is diameter of orifice and U is the average stroke expulsion velocity from the orifice, and C is equal to 0.16.

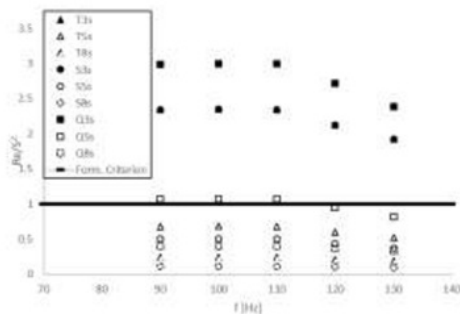


Fig. 8: Synthetic Jet Formation Criteria

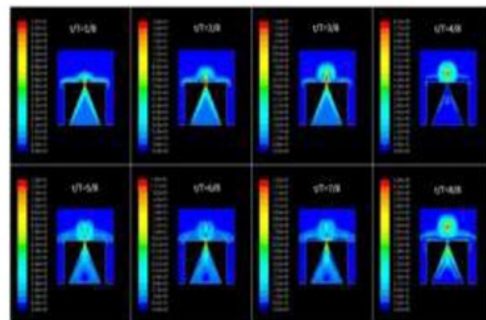


Fig. 9: Vortex Ring Simulation Sinusoidal Wave 110 Hz

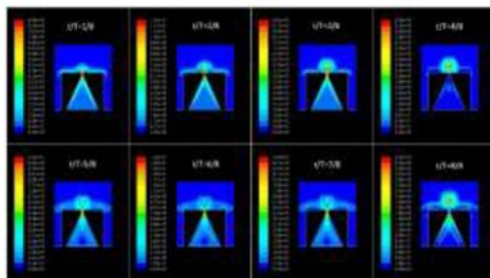


Fig. 10: Vortex Ring Simulation Triangle 110 Hz

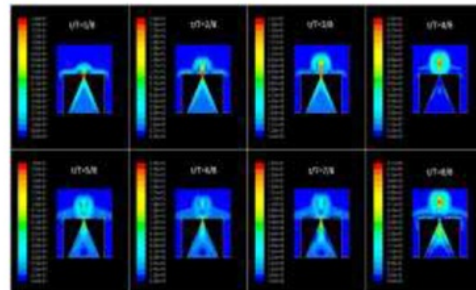


Fig. 11: Vortex Ring Simulation Square Wave 110 Hz

Then, this Holman criteria in Figure 8 explains that the square wave signal of actuator can produce the higher vortex ring formation than the other type of signal. [9] In addition, Figure 9 explains that the Holman criteria theory is proven, when the 10 Hz square wave signal is applied to the 3 mm orifice diameter conical synthetic jet, the expulsion stroke of vortex ring velocities is 5.71 m/s. Meanwhile, In Figure 9 and 10 explain that other type of signal applied to the 3 mm conical synthetic jet produces 4.36 m/s of expulsion stroke for sinusoidal wave and 3.36 m/s of air stroke for triangle wave.

3.2. The Airflow Separation Condition After the Application of Synthetic Jet Orifice Diameter 3 mm, 5 mm, and 8 mm

3.3. A Free Stream velocity 11.1 m/s

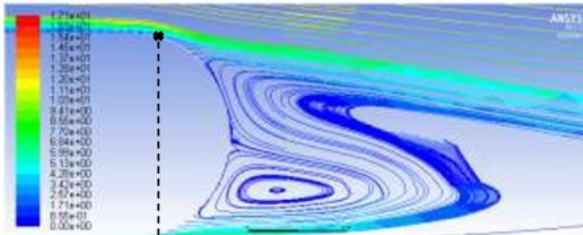


Fig. 12: Separation Point without Synjet Jet Square wave

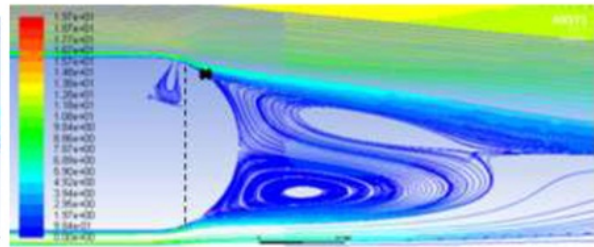


Fig. 13: Separation Point 3 mm Synthetic jet square

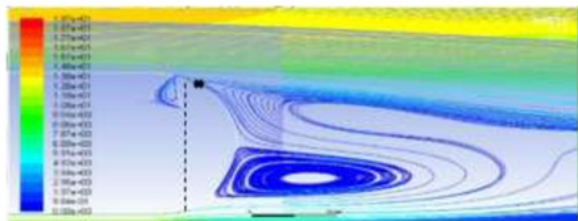


Fig 14: Separation point 5 mm Synthetic Jet Square Wave

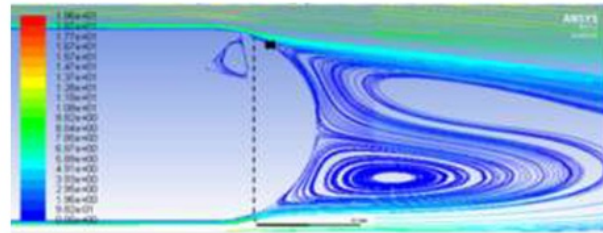


Fig. 15: Separation point 8 mm Synthetic Jet Square Wave

Figure 12 shows that the airflow separation happens at (635,196) from the point origin (0,0). Then, if it is compared to the synthetic jet which diameter 5 mm and 8 mm the longest distance of airflow separation postponement is 3 mm cavity orifice synthetic jet. Based on the figure 13 the separation point is moved to (649,182) mm.

3.4. Free Stream Velocity 13.9 m/s

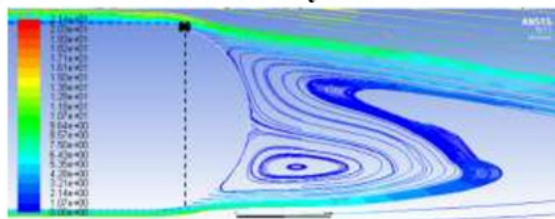


Fig. 16: Airflow Separation without Synjet at 13.9 m/s

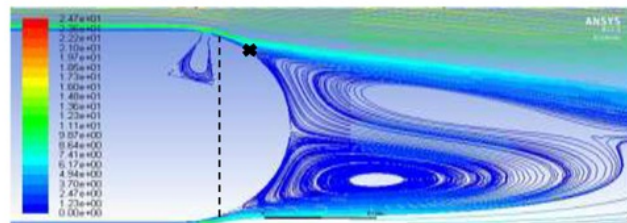


Fig. 17: Separation point 3 mm Synthetic Jet Square Wave

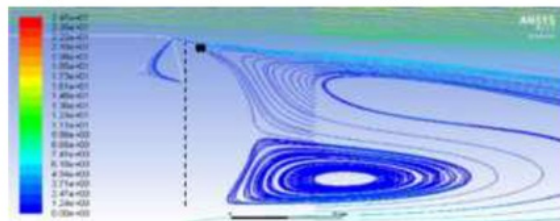


Fig. 18: Separation point 5 mm Synthetic Jet Square Wave

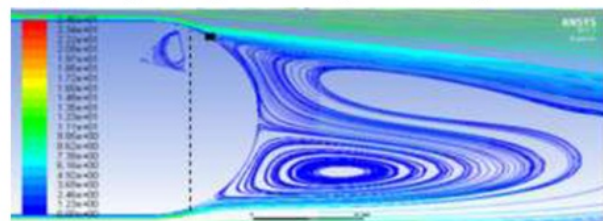


Fig. 19: Separation point 8 mm Synthetic Jet Square Wave

When the free stream 13.9 m/s and there is no synthetic jet applied, it can be seen from figure 16 that the airflow separation happens at (633,198)mm from x,y=(0,0). Furthermore, the figure 17 explains that the maximum airflow separation postponement happens when the synthetic jet actuator 3 mm applied, the separation point become (651,190) mm from the origin point.

3.5. At the Free Stream Velocity 16.7 m/s

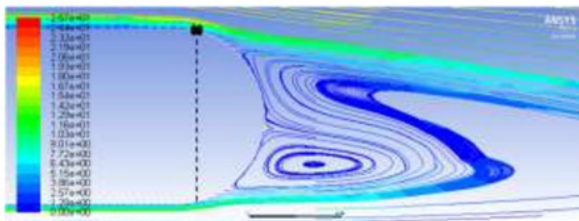


Fig. 20: Airflow separation point at Free stream 16.7m/s

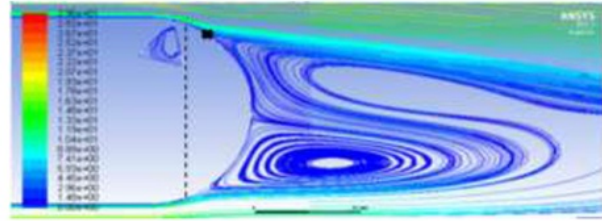


Fig. 21: Separation point 3 mm Synthetic Jet Square Wave

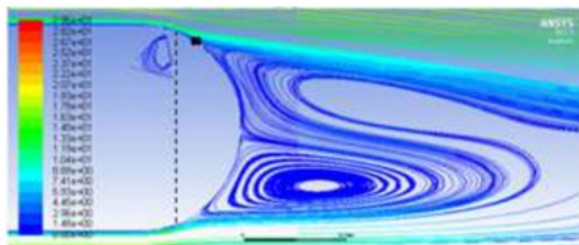


Fig. 22: Separation point 5 mm Synthetic Jet Square Wave

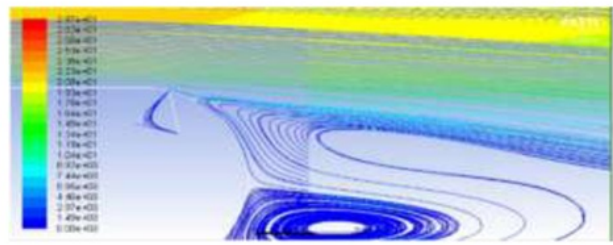


Fig. 23: Separation point 8 mm Synthetic Jet Square Wave

As the free flow get faster than before from 13.9 m/s to 16.7 m/s, the airflow separation will get early to happens [10] and Figure 20 shows that the airflow separation happens at (631,200)mm. When the synthetic jet actuator which orifice diameter 3 mm applied to this model. Figure 21 explains that the maximum airflow separation postponement happens and it becomes (643,188)mm from the origin point.

3.6. Drag Force Reduction

3.7. Drag Force Reduction at Free Stream 11.1 m/s

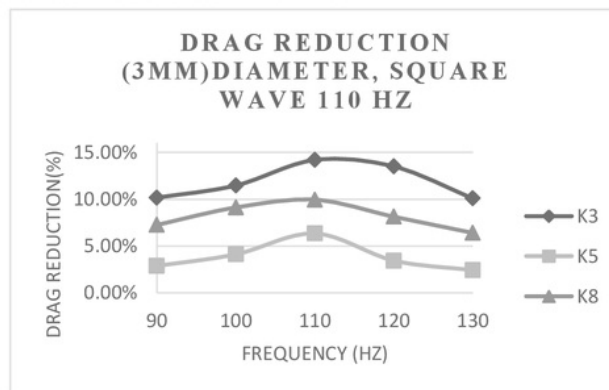


Fig. 24: Drag Reduction Percentage of Conical Cavity Orifice Diameter 3 mm, 5 mm, 8 mm

Figure 24 explain about the drag reduction through the variation of orifice diameter in free stream velocity 11.1 m/s. As it can be seen from the graph above in the 3 mm orifice diameter produces the highest drag reduction 14.2% then it follows by 5 mm orifice diameter which the drag reduction 9.95% and 8 mm orifice diameter which drag reduction is 6.35%.

3.8. Drag Force Reduction at Free Stream 13.9 m/s

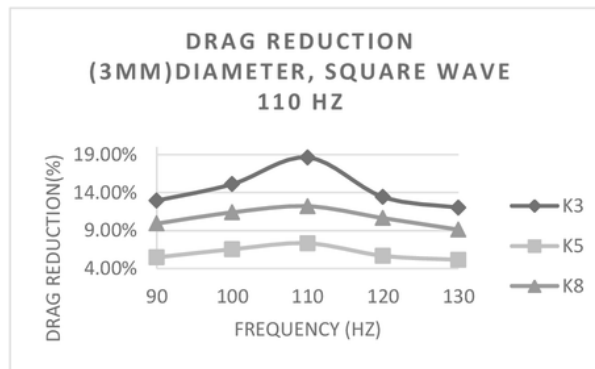


Fig. 25: Drag Reduction Percentage of Conical Cavity Orifice Diameter 3 mm, 5 mm, 8 mm

Figure 25 above explains that drag reduction of all three types orifice diameter of conical cavity synthetic jet are rising. The 3 mm diameter has 18.62%, 5 mm has 12.21% and 8 mm has 7.34% of drag force reduction.

3.9. Drag Force Reduction at Free Stream 16.7 m/s

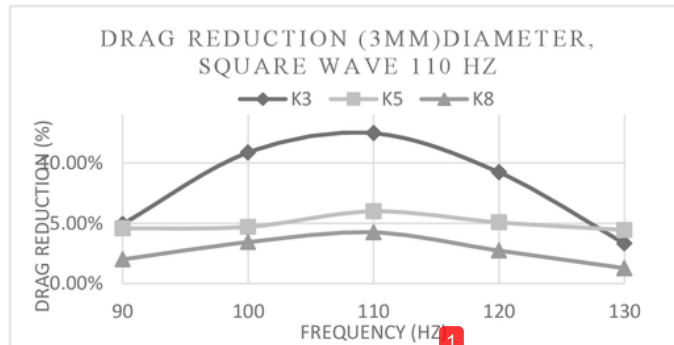


Fig. 26: Drag Reduction Percentage of Conical Cavity Orifice Diameter 3 mm, 5 mm, 8 mm

The graph in figure 26, explains different things happens because on the figure 24 and 25 shows that as the velocity rises the drag reduction increase. In this free stream the 3 mm of conical cavity drag reduction is 12.48 and still remain the highest, then it follows by 5 mm which reduction is 5.99% and 8 mm diameter has 4.24 of drag reduction.

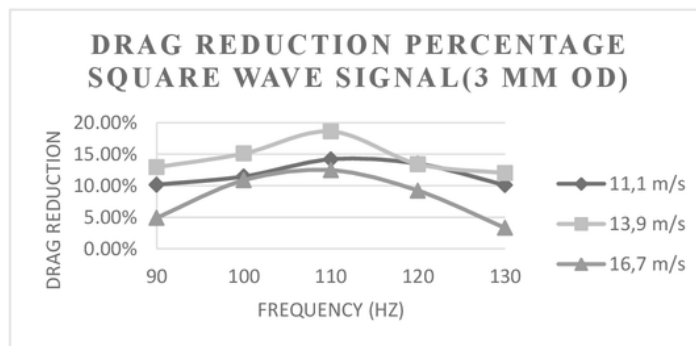


Fig. 27: Drag reduction Percentage of 3 mm diameter conical synthetic jet

Figure 27 explains that the smallest drag reduction happens when the 3 m orifice diameter of conical cavity synthetic jet applied the free stream velocity 16.7 m/s. Based on the fluid mechanics theory, as the free flow get

risers, the airflow separation will get earlier to happens, so the drag force produced is high. [11]Furthermore, since the point to take the separation poin is fixed, whether the model is not applied or applied with the synthetic jet actuator, so it is reasonable that the higher the velocity stream, the smaller drag force reduction will be.

3.10. Conclusion

Based on the simulation result, the maximum drag force reduction ¹ produced by the 3 mm ¹ orifice diameter of conical cavity syntheti¹ jet when the membrane actuator vibrate at 110 hz of square signal wave and the free stream velocity is 13.9 m/s. The amount of drag force reduction is 18.62%.

4. Acknowledgements

This paper would not be possible to finish without the support from my institution, University of Indonesia and the research grants from research development of University of Indonesia (PITTA). In addition the author also indebt to all of these person in charge who always support me during the process of finishing the paper:

1. Prof. Dr. Ir. Harinaldi, M.Eng, as the author professor project advisor. The author thanks for his time to guide the author for finishing this projects
2. Ramon Trisno, S.T, M.Eng, as the research promotor, because of his help to take the experiment and simulation data, the time to share his knowledge about the research, this project finish before the due date.
3. The research team, Helmy Azis, Bisma Kertanegara, Bintang Antares and Rizki Abdul Azis, who already give their time to share the knowledge and experience for discussing our final project.

The author sincerely wishes this paper could be useful to its readers by giving valuable information. The author fully realizes all the imperfection inside this final project. Therefore, the author humbly requests for the readers' criticism, feedback and suggestions to improve our future reports. We also apologize if there is any mistakes in this paper.

5. References

- [1] Munson, B, Fluid Mechanics(Translated by :Prof.Dr.Ir.Harinaldi & Ir.Budiarso, M.Eng), Jakarta: Erlangga, 2002.
- [2] Olson R.M and Wright S.J, Basic Fluid Mechanics(Translated by: Alex Tri Kantjono), Jakarta: PT Gramedia Pustaka, 1993.
- [3] M. Gak-El-Hak, "Modern Development in Flow Control,," *Appl. Mech. Rev.*, 9, pp. 365-379, 1996.
<https://doi.org/10.1115/1.3101931>
- [4] G. R. a. G. F. Ahmed S.R., *Airflow Study Through Ahmed body Model*, no. 8400300-01, 1984.
- [5] Versteeg & Malalasekera, *Computational Fluid Dynamic The Finite Volume Method.*, England: Longman, 1996.
- [6] Jiyuan Tu, Guan Heng Yeoh, Chaoqun Liu, *Computational Fluid Dynamics, A Practical Approach*, Oxford: Elsavier, 2008.
- [7] Ansys Inc, *Introduction To Ansys Meshing*, USA: ANSYS, 2014.
- [8] Brunn A., Wassen, Sperber D, Nitsche W, and Thiele F, "Active Drag Control for a Generic Car Model," *Active Flow Controk*, no. 95, pp. 247-259, 2007.
- [9] Y. U. R. M. B. S. L. C. R. Holman, " 'Formation criterion for synthetic jets'," *AIAA Journal*, vol. 43, no. 10, p. 2110-2116., 2005.
<https://doi.org/10.2514/1.12033>
- [10] 2. Fares E., "Unsteady flow simulation of the Ahmed reference body using a lattice Boltzmann approach," *Computers, and Fluids*, vol. 35, pp. 940-950, 2006.
<https://doi.org/10.1016/j.compfluid.2005.04.011>
- [11] Roumeas M, Gillieron, and Kourta A, "Analysis and Control Of the Near Wake Flow Over a Square Back Geometry," *Computers & Fluids*, pp. 60-70, 2009.
<https://doi.org/10.1016/j.compfluid.2008.01.009>
- [12] Lienhart H, Stoots C, and Becker S, *Flow and Turbulence Structure in The Wake Of a Simplified Car Model(Ahmed Model), Numerical and Experimental Fluid*, 2002.

Computational Analysis Orifice Diameter Variations Effects of Conical Cavity Synthetic Jet Actuator on the Drag Force Reduction Percentage of the Reversed Ahmed Body Model

ORIGINALITY REPORT

12%

SIMILARITY INDEX

5%

INTERNET SOURCES

9%

PUBLICATIONS

3%

STUDENT PAPERS

PRIMARY SOURCES

- 1** Harinaldi, Ramon Trisno, Bisma Kertanegara. "The Effect of Orifice Diameter Variations of Conical Cavity Synthetic Jet Actuator on the Drag Reduction of the Reversed Ahmed Body Model", Proceedings of the 2017 International Conference on Industrial Design Engineering - ICIDE 2017, 2017 7%

Publication
- 2** Submitted to University of Stellenbosch, South Africa 1%

Student Paper
- 3** eacbee.org 1%

Internet Source
- 4** Submitted to The Robert Gordon University 1%

Student Paper
- 5** media.neliti.com 1%

Internet Source

Submitted to Laureate Education Inc.

6

Student Paper

1%

7

www.scribd.com

Internet Source

<1%

8

ntrs.nasa.gov

Internet Source

<1%

Exclude quotes On

Exclude matches < 10 words

Exclude bibliography On